Synthesis, structural and luminescence properties of Dy^{3+} activated GdAlO$_3$ phosphors by a solid state reaction method under a N$_2$ atmosphere

SAMIT TIWARI[1], **RAUNAK KUMAR TAMRAKAR**[1,*], **KANCHAN UPADHYAY**[2] **and C S ROBINSON**[1]

[1]Department of Applied Physics, Bhilai Institute of Technology (Seth Balkrishan Memorial), Near Bhilai House, Durg (C.G.) 491001, India

[2]International and Inter University Centre of Nanoscience and Nanotechnology, Mahatma Gandhi University, Kottayam 686560, India

*Author for correspondence (raunak.ruby@gmail.com)

Abstract. Dysprosium (Dy^{3+}) ion-doped GdAlO$_3$ nanophosphors were fabricated by using a high temperature solid state reaction method. X-ray diffraction measurements were used to investigate the phase and crystal size of these phosphors. The morphology of the powder was observed by scanning electron microscopy. The band structure of the phosphor was determined by recording the UV absorption spectra and Tauc plot. The optical behaviour of the phosphors was determined by measuring their photoluminescence (PL) spectra. The PL spectra show characteristic blue (489 nm) and green (567 nm) emissions corresponding to the energy level transitions of Dy^{3+}.

Keywords. GdAlO$_3$; Dy^{3+}; XRD; photoluminescence; CIE.

1. Introduction

Perovskite compounds behave as the best host materials for the development of various display devices. The perovskite compound has the general formula of ABO$_3$. Gadolinium aluminate belongs to the perovskite structure-based compound. It has an orthorhombic crystal structure that belongs to the *Pm*3*m* symmetry group. Perovskites are chemically and thermally stable, which makes them very useful for various applications [1–4]. Doping of Dy^{3+} ions in the GdAlO$_3$ host makes it useful for white light applications. Dy^{3+} ions are active rare earth ions for the production of white light. Due to this, they are one of the most studied rare earth ions [5,6]. The emission of Dy^{3+} ions can be tuned by varying the host matrix [7,8].

Various preparation methods have been used for the synthesis of GdAlO$_3$ phosphors doped with various rare earth ions, which include solvothermal, combustion synthesis, solid state reaction, etc. In the present study the structural and luminescence properties of different concentrations of Dy^{3+} activated GdAlO$_3$ nanophosphors by means of a solid state reaction method under a N$_2$ atmosphere have been studied.

2. Synthesis

The GdAlO$_3$:Dy^{3+} phosphors have been synthesized by the solid state reaction method already developed for Er^{3+}:Yb^{3+}-codoped GdAlO$_3$ phosphors by replacing the oxides of erbium and ytterbium with dysprosium oxide (Dy$_2$O$_3$) [9]. To determine the influence of the dopant concentration on the spectral behaviour, phosphors with variable Dy^{3+} concentrations have been prepared by using the above-mentioned method.

3. Results and discussion

3.1 *Phase, structure and morphology*

Figure 1 shows the X-ray diffraction (XRD) patterns of the sample. The obtained XRD pattern of the sample matches well with the JCPDS file No. 46-0395 [10,11] indicating that the sample has an orthorhombic phase. No other peaks due to Dy^{3+} are observed in the XRD pattern revealing that the sample has a pure phase of GdAlO$_3$. The average crystal size of the phosphor was determined by using Scherer's formula [12]. The crystal size obtained was around 59 nm.

The bonding behaviour of the sample was determined by recording the Fourier-transform infrared (FTIR) spectra (figure 2). A strong absorption peak at 549.86 cm^{-1} corresponds to the Gd–O vibrational modes [13].

The surface morphology of the phosphor was determined by scanning electron microscopy (SEM) analysis (figure 3). The image shows agglomeration. This agglomeration is due to the high-temperature profile. The crystal size obtained from the XRD results was further confirmed by using the
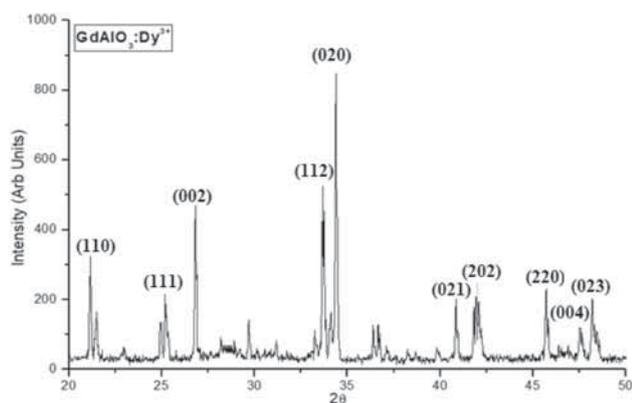
Figure 1.   XRD patterns of Dy^{3+} activated $GdAlO_3$ phosphors.

transmission electron microscopy (TEM) image. Figure 4 shows the TEM image of the phosphor. It confirms that the particle size is around 67 nm, which is in agreement with the XRD result.

3.2   *Band structure of the sample*

The band structure of the prepared phosphor and its variation with the dopant concentration was studied by recording the absorption spectra of the sample with variable Dy^{3+} concentrations. It was observed that the absorption wavelength shifts towards the higher wavelength side with an increase in the Dy^{3+} concentration. The absorption wavelength was obtained at 277, 295 and 306 nm for 0.5, 1 and

1.5 mol% of Dy^{3+} concentration, respectively (figures 5). The absorption edge of the sample represents the band gap of the crystal which was determined by using the Tauc plot [14]. The band gap energy values were found to be 5.6, 5.73 and 5.92 eV for 0.5–1.5 mol% Dy^{3+}, respectively (figure 6). The change in the band gap is due to the increase in the carrier concentration [15].

3.3   *Optical properties*

To study the optical behaviour of the phosphor, the emission spectra of Dy^{3+} doped $GdAlO_3$ were recorded under 256 nm excitation. The emission spectrum has characteristic peaks of Dy^{3+} ions. The emission peaks were centred in the blue region at 489 nm along with an intense green emission centred at 567 nm (figure 7). The characteristic emission centred at 489 nm corresponds to $^4F_{9/2} \rightarrow {}^6H_{15/2}$ and 567 nm corresponds to $^4F_{9/2} \rightarrow {}^6H_{13/2}$. The blue emission is due to the magnetic dipole interaction whereas the yellow emission is due to the electrical interaction [16].

The effect of Dy^{3+} ion concentration on the emission spectra were determined as a function of variable Dy^{3+} concentration. The emission intensity increases with an increase in Dy^{3+} concentration up to 1.25 mol% and after this concentration the intensity decreases. This decrease in intensity is due to the concentration quenching (figure 7). The increase in the intensity with an increase in Dy^{3+} concentration is due to the decrease in the average interionic distance between nearby Dy^{3+} ions, which enhances the cross relaxation process. The cross relaxation is responsible for de-excitation of $^4F_{9/2}$ to $^6H_{15/2}$ and excites the nearby Dy^{3+} ions $^6F_{3/2}$, $^6F_{7/2}$ or $^6H_{9/2}$
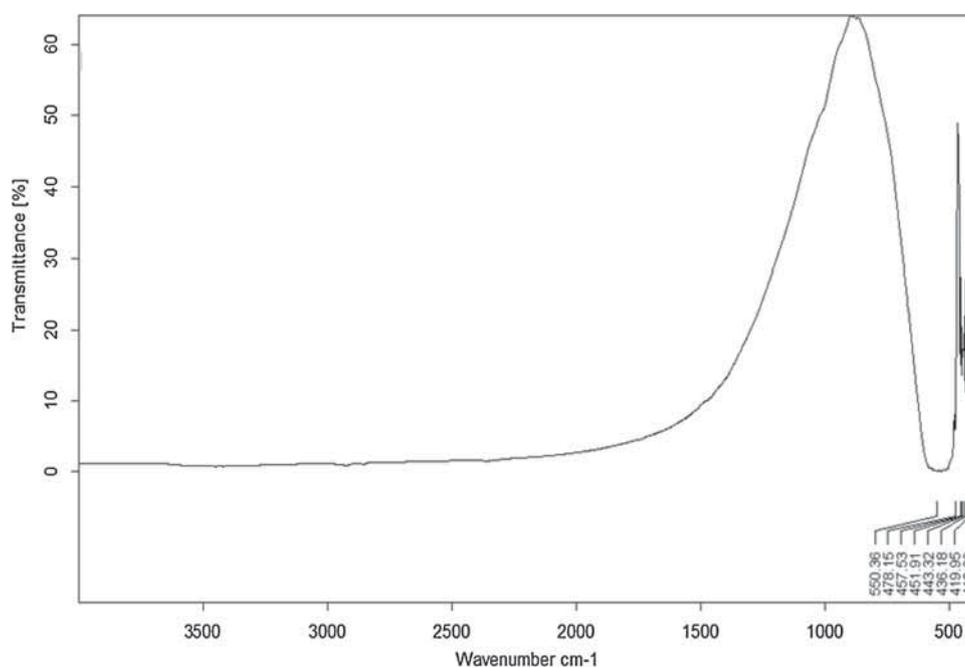
Figure 2.   FTIR image of Dy^{3+} activated $GdAlO_3$.

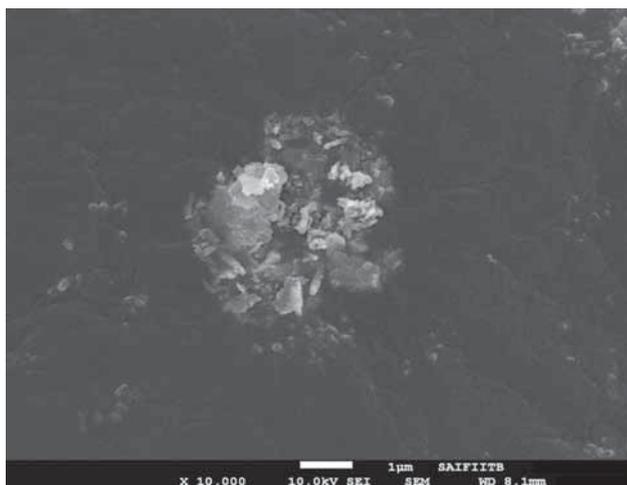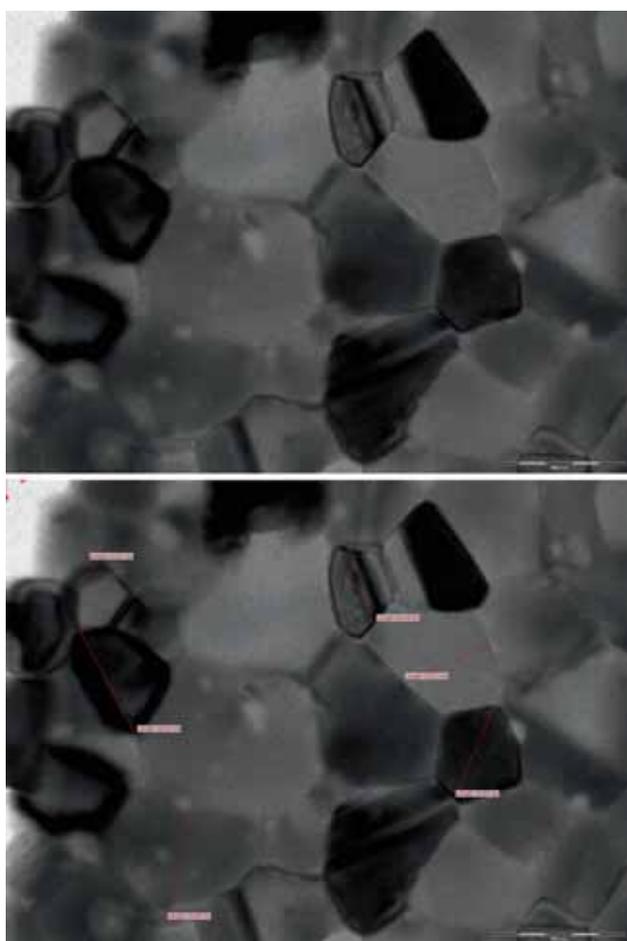**Figure 3.** SEM image of Dy^{3+} activated GdAlO$_3$.

Figure 5. Absorption spectra of the GdAlO$_3$:xDy^{3+} (x = 0.5, 1 and 1.5 mol%).

Figure 4. TEM image of Dy^{3+} activated GdAlO$_3$.
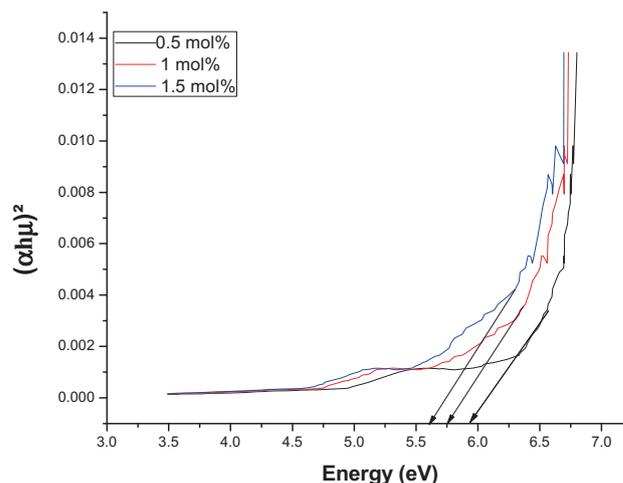
Figure 6. Tauc's plot of the GdAlO$_3$:xDy^{3+} (x = 0.5, 1 and 1.5 mol%).

3.4 *CIE chromaticity*

The final emitted colour of the prepared phosphor was determined by using the CIE colour coordinates. The X and Y coordinates were determined by using the colour chromaticity diagram using MATLAB 7.10.0 software. The X and Y coordinates have values 0.365 and 0.457, respectively, which correspond to the yellowish green emission (figure 8).

3.5 *GdAlO$_3$:Dy^{3+} photoluminescence decay*

Figure 9 shows the typical PL decay curves of the GdAlO$_3$: Dy^{3+} phosphor. The initial afterglow intensity of the material was high. The decay times of phosphors can be calculated by using a curve fitting technique, and the decay curves fitted by

levels. After a particular concentration the $^6F_{9/2}$ level of all Dy^{3+} is involved in cross relaxation, resulting in the quenching of emission due to the $^6F_{9/2}$ level [17–20].
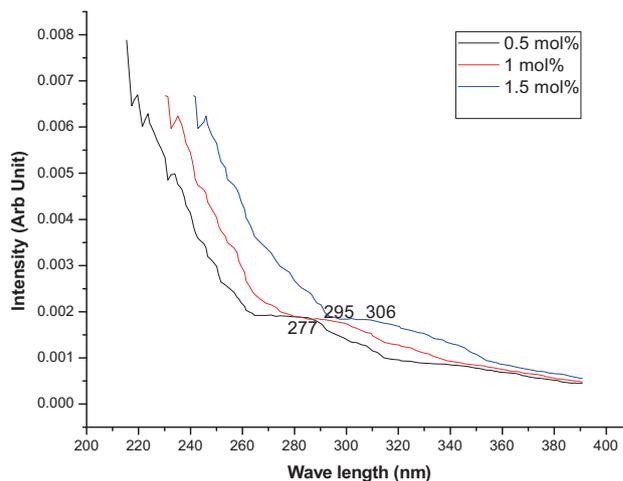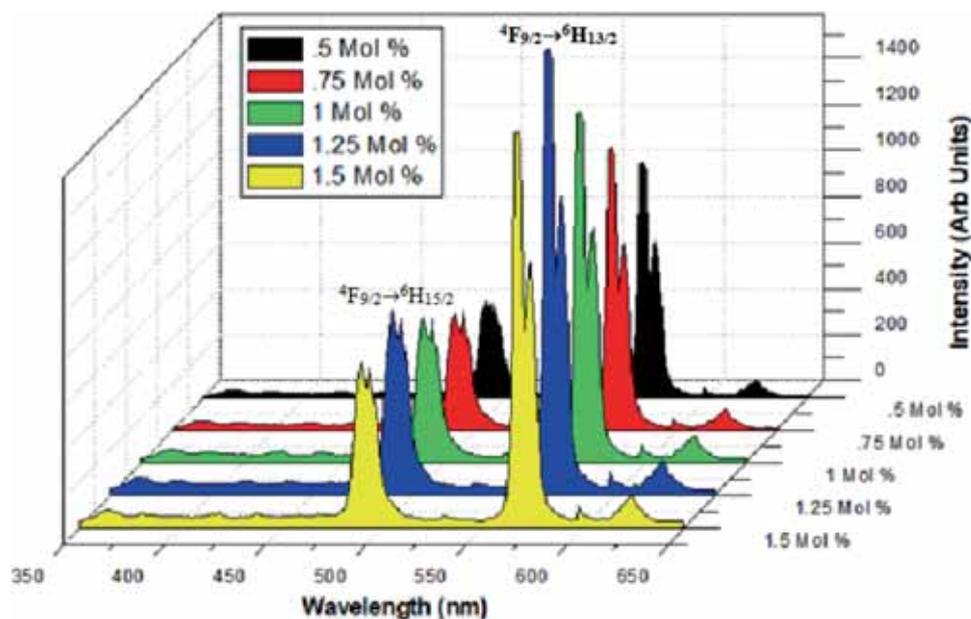
Figure 7. Effect of Dy^{3+} ion concentration on $GdAlO_3$ PL emission intensity under 256 nm excitation.
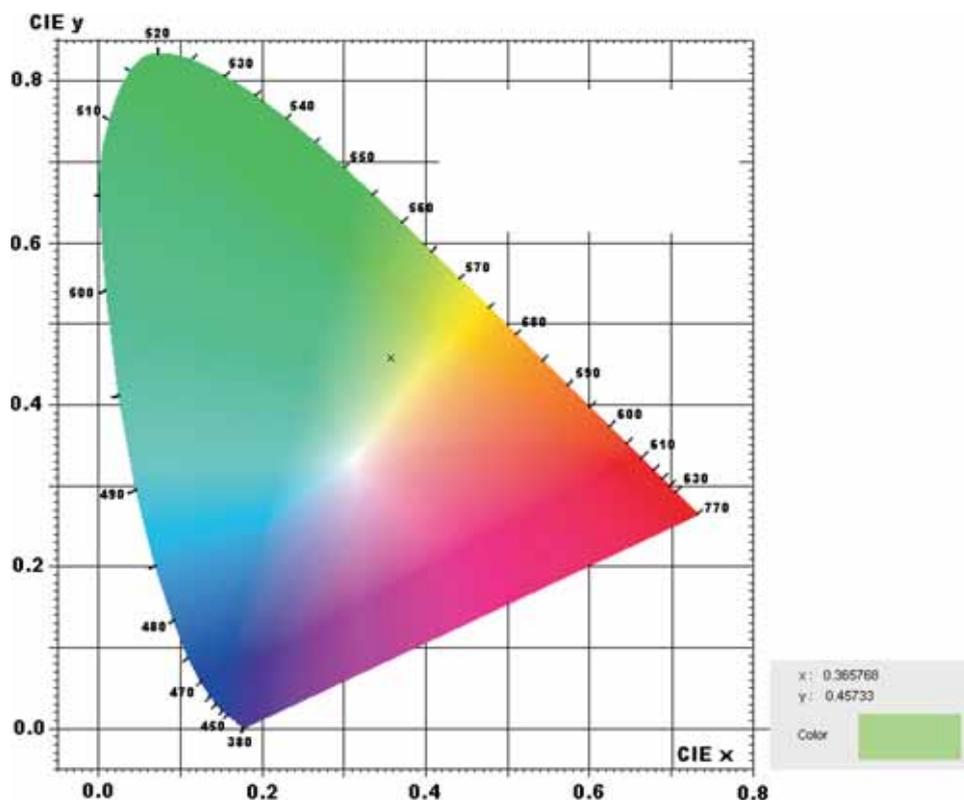

Figure 8. CIE diagram of $GdAlO_3:Dy^{3+}$.

the sum of two exponential components have different decay times.

$$I = A_1\exp(-t/\tau_1) + A_2\exp(-t/\tau_2) \qquad (1)$$

where I is the phosphorescence intensity, A_1 and A_2 are constants, t is the time and τ_1 and τ_2 are decay times (in nanoseconds) for the exponential components. Decay curves are successfully fitted by equation (1). The fitting
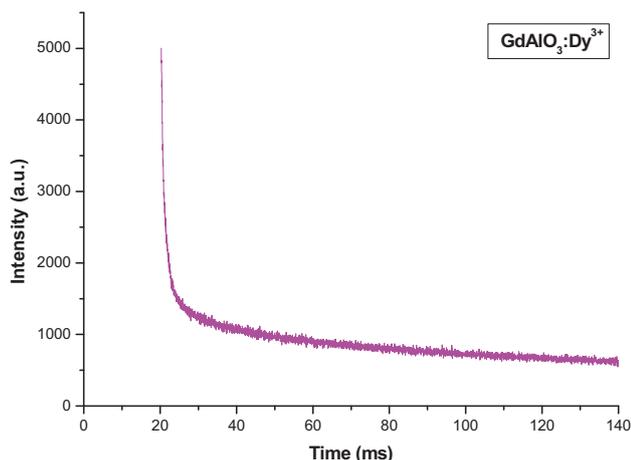
Figure 9. Decay curves of $GdAlO_3:Dy^{3+}$ phosphor.

Table 1. The fitting result of the decay curves.

Sample	τ_1 (ms)	τ_2 (ms)
$GdAlO_3:Dy^{3+}$	1.36	61.32

results of decay curves are shown in table 1.

Alkaline earth ion sites are a very probable source of electron trap. In the alkaline earth silicate, most of the excitation energies will be transferred from the host ($Dy^{3+} \rightarrow$ host). However, part of the excitation energy will be stored when some of the excited carriers drop into the traps, instead of returning to the ground states. Later, the traps created by Dy^{3+} are deeper and on thermal excitation at suitable temperature; these carriers will be released from the traps and transferred *via* the host to the Dy^{3+} ions, followed by the characteristic Dy^{3+} emissions as long afterglow. Dy^{3+} in the silicates act as traps, meanwhile Dy^{3+} can also act as luminescence centres [21–23].

4. Conclusion

The solid state reaction method has been used for synthesizing Dy^{3+} doped $GdAlO_3$ phosphors. XRD analysis of the phosphor revealed that the phosphor has a cubic structure. The crystal size obtained was around 59 nm. XRD patterns and TEM analysis also revealed the particle size to be around 67 nm, which is in good agreement with the XRD results. The emission spectra recorded under 256 nm excitation show strong emission peaks in yellow and blue regions. CIE chromaticity confirms the emission in the green region. The maximum intensity was obtained for 1.25 mol% of Dy^{3+} ion concentration.

References

[1] Tamrakar R K and Upadhyay K 2016 *J. Disp. Tech.* **12** 599
[2] Dhahri K 2014 *Mater. Lett.* **128** 235
[3] Shilpa C J 2014 *Spectrochim. Acta Part A: Mol. Biomol. Spectrosc.* **133** 550
[4] Medeiros I S, Yoshimura H N L, Cesar P F and Hernandes A C 2009 *J. Mech. Behavior Biomed. Mater.* **2** 471
[5] Phaomei G, Singh W R and Ningthoujam R S 2011 *J. Lumin.* **131** 1164
[6] Singh N S, Ningthoujam R S, Phaomei G, Singh S D, Vinu A and Vatsa R K 2012 *Dalton Trans.* **41** 4404
[7] Shanmugavelu B and Kumar V V R K 2014 *J. Lumin.* **146** 358
[8] Wang G Q, Gong X H, Chen Y J, Huang J H, Lin Y F, Luo Z D *et al* 2014 *Opt. Mater.* **36** 1255
[9] Tamrakar R, Upadhyay K and Sahu M 2016 *J. Alloys Compd.* **689** 702
[10] Wang P 1994 *Shanghai Inst. of ceramics, Chinese Academy of Science* (Shanghai, China, ICCD grant-in-Aid)
[11] Oliveira H H S, Cebim M A, Da Silva A A and Davolos M R 2009 *J. Alloys Compd.* **488** 619
[12] Guinier A 1963 *X-Ray Diffraction* (San Francisco, Calif, USA: Freeman)
[13] Tamrakar R K, Bisen D P, Sahu I P and Brahme N 2014 *J. Radiat. Res. Appl. Sci.* **7** 417
[14] Lopez R and Gomez R 2012 *J. Sol–Gel Sci. Technol.* **61** 1
[15] Saha B, Das S and Chattopadhyay K K 2007 *Sol. Energy Mater. Sol. Cells* **91** 1692
[16] Baéz-Rodrígueza A, Alvarez-Fragosob O, García-Hipólitob M, Guzmán-Mendozac J and Falcony C 2015 *Ceram. Int.* **41** 7197
[17] Parisi D, Toncelli A, Tonelli M, Cavalli E, Bovero E and Belletti A 2005 *J. Phys. Condens. Matter* **17** 2783
[18] Tamrakar R K and Upadyay K 2017 *Int. J. Lumin. Appl.* **7** 374
[19] Tamrakar R K and Upadyay K 2018 *Opt. Quant. Electron.* **50** 271
[20] Tamrakar R K, Upadyay K and Bisen D P 2016 *Infrared Phys. Technol.* **75** 160
[21] Verweij J W M *et al* 1995 *Chem. Phys. Lett.* **239** 51
[22] Cizauskaite S *et al* 2007 *Mater. Chem. Phys.* **102** 105
[23] Shanta Singh N, Ningthoujam R S, Yaiphaba N, Dorendrajit Singh S and Vatsa R K 2009 *J. Appl. Phys.* **105** 064303